Moderate Resolution Imaging Spectroradiometer (MODIS) Downward Shortwave Radiation (MCD18A1) and Photosynthetically Active Radiation (MCD18A2) User Guide

Collection 6

Dongdong Wang, Shunlin Liang

Department of Geographical Sciences

University of Maryland, College Park

September 2017

Contents

1. Introduction

Incident solar radiation over land surfaces, either photosynthetically active radiation (PAR) in the visible spectrum (400-700nm) or downward shortwave radiation (DSR) in the shortwave spectrum (300-4000nm), is a key variable to address a variety of scientific and application issues related to climate trends, hydrologic, bio-physical and bio-chemical modeling, solar energy applications, and agriculture.

Data of DSR and/or PAR are required by almost all land models, such as driving photosynthesis, modeling carbon cycling, analyzing hydrological and energy balance, weather and climate prediction. The DSR and PAR data also find their use in many application areas, including agricultural management, ecological forecasting, reusable energy production, public health and so on. The current global satellite products of surface radiative fluxes usually have rather coarse spatial resolutions, such as the Clouds and the Earth's Radiant Energy System (CERES) product at a spatial resolution of 140km from 1997 to present, the International Satellite Cloud Climatology Project (ISCCP) product on a 280 km equal-area global grid from 1983-2008, the Global Energy and Water Cycle Experiment (GEWEX) surface radiation budget (SRB) product at a spatial resolution of 1° x 1° from 1983-2007. Besides, few land surface global PAR products exist because most global radiative flux datasets do not include PAR, so users have to empirically convert DSR to PAR. The conversion itself is a source of uncertainties.

The high-quality DSR and PAR products with finer spatial resolution will enable us to better model these processes and provide us better understanding to a series of critical Earth science and application questions. For example, these products with high spatial resolution are especially needed for land applications, such as generating high-resolution terrestrial gross and net primary production (GPP/NPP) Earth Science Data Record (ESDR), evapotranspiration (ET) ESDR. However, there is no high-resolution global land surface DSR or PAR ESDR available, although high-resolution global ocean PAR ESDR (9.3km) has been generated through the NASA MEaSUREs Program

Funded by NASA, a suite of global 5km DSR and PAR products over land surfaces are generated from MODIS data. Compared to other existing products, the new products represent substantial improvement over spatial resolution. The new product suite is consisted of two gridded L3 products: MCD18A1 (Downward Shortwave Radiation) and MCD18A2 (Photosynthetically Active Radiation). MCD18A1 and MCD18A2 are combined Aqua and Terra MODIS products. This user guide will document the technical details of data files and scientific data sets of the products. It will also briefly describe the theoretical basis and practical consideration of the retrieval algorithm.

2. Algorithm summary

The basic framework of the algorithms was presented by Liang et al. (2006) for estimating PAR. The algorithm first estimates surface reflectance from multi-temporal imagery and then appraises

PAR flux for each imagery. The major procedure is composed of two steps: (1) determination of the surface reflectance from observations under the “clearest” atmospheric conditions in a temporal window; and (2) calculation of incident PAR from the determined surface reflectance and TOA radiance/reflectance using the LUT approach. The LUTs consider different types and loadings of multiple aerosols and clouds at a variety of illumination/viewing geometry. The key concept of this algorithm is use of multi-temporal signatures of MODIS data (Figure 1).

In the follow-up studies, a series of refinements and improvements have been made. For example, MODIS surface reflectance product (MOD09) was used to map PAR over China from MODIS data (Liu et al. 2008). It has been extended to estimate PAR from GOES data (Zheng et al. 2008) by taking into account topographic effects. It was also extended to estimate DSR over China from Geostationary Meteorological Satellite (GMS) 5 imagery by considering water vapor and the surface elevation (Lu et al. 2010). Huang et al. (2011) further extended the LUT scheme to estimate DSR by combining the Multifunctional Transport Satellite (MTSAT) data and MODIS data products.

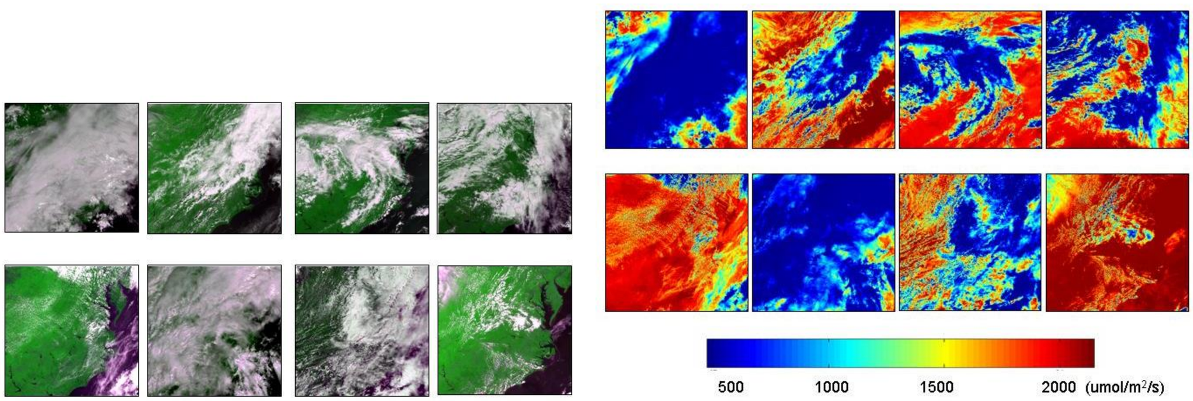

Figure 1. Time series of MODIS observations of TOA radiance and the derived surface incident PAR results.

Based on these studies, the extensive prototyping has also been carried out for producing global DSR and PAR products (Zhang et al. 2014). The key feature of the prototyping algorithm is the use of DSR and PAR LUTs for different types and loadings of aerosols and clouds. It consists of several key steps:

1) The satellite TOA radiance/reflectance for different sensors is calculated based on the digital numbers (DN values) using the calibration coefficients.
2) The surface reflectance is derived for different sensors. The MODIS land surface reflectance product is used as the input parameter for the MODIS sensor. However, for geostationary and AVHRR satellite data, the minimum TOA reflectance method is employed to derive the surface reflectance.
3) TOA radiance is estimated for each atmospheric condition from the clearest condition to the cloudiest conditions (high cloud extinction coefficient) based on the first LUT in

Figure 2. Then, the actual TOA radiance calculated from the sensors is compared to the series of the simulated radiance for different atmospheric conditions to retrieve the atmospheric index.

4) DSR and PAR from each sensor are estimated by searching the second LUT in Figure 2 using the estimated atmospheric condition index and surface reflectance.
5) A Bayesian procedure is used to integrate estimates of MODIS and geostationary satellite data and the probability is determined based on extensive validation using in-situ measurements.

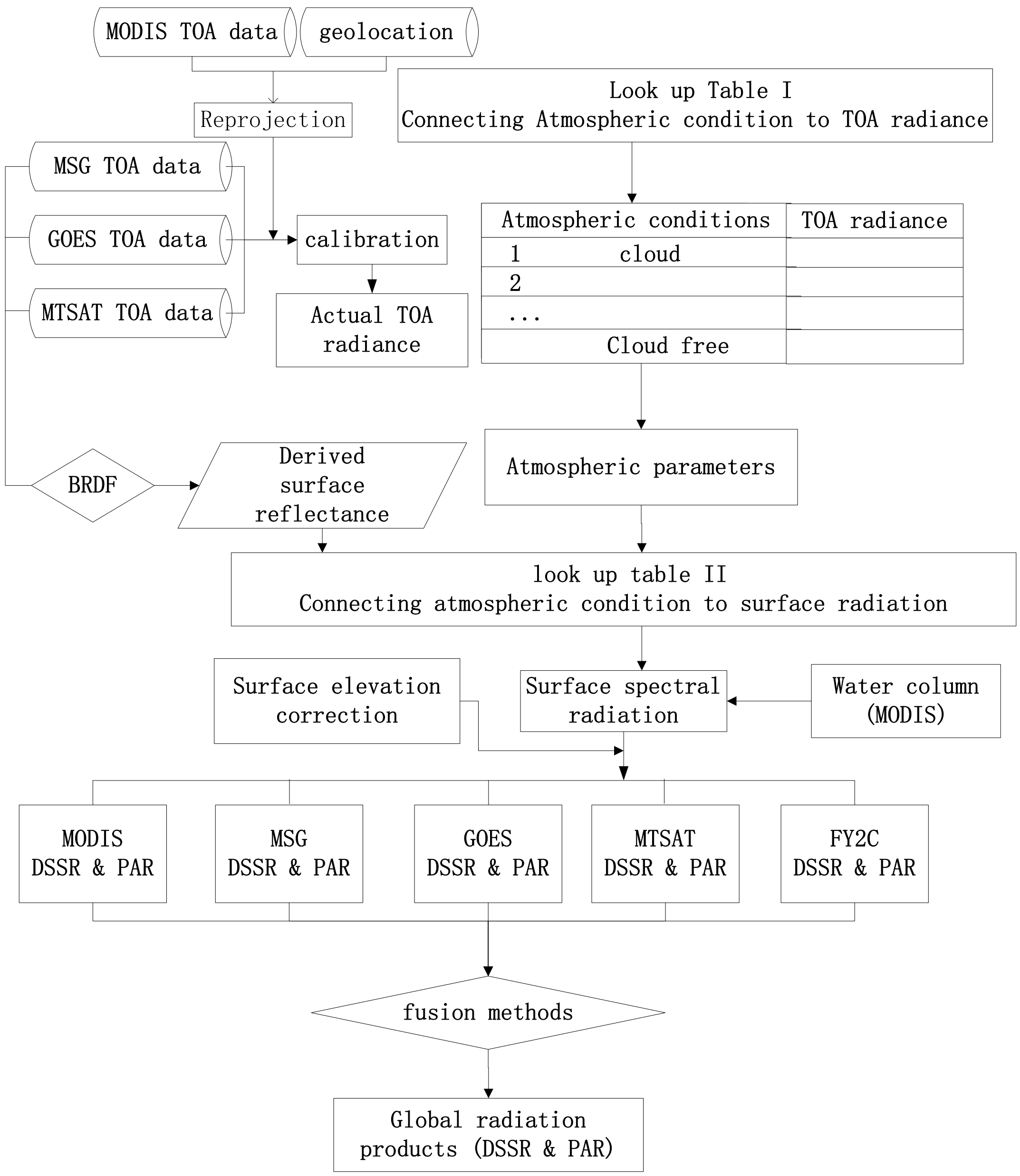

Figure 2. Flowchart to generate global DSR and PAR products from MODIS and geostationary satellite data

Although data of geostationary satellites were included in the prototype system, the current version DSR and PAR products (Collection 6) use only MODIS data because of practical consideration. MODIS/Terra and MODIS/Aqua data are used, which provide a daily coverage over most of the world (Figure 3).

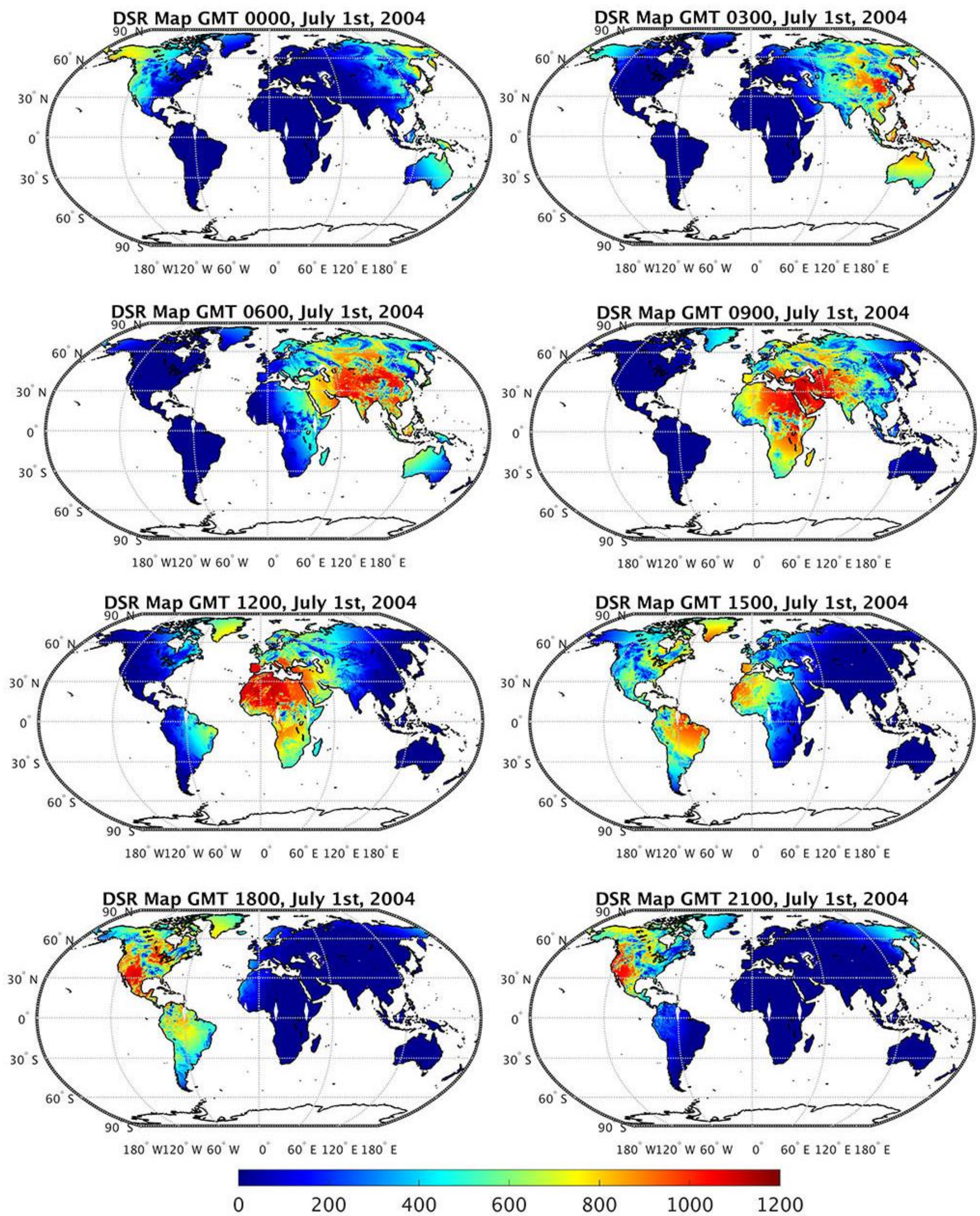

Figure 3. Global maps of 3-hourly DSR of July 1 2004 generated from MODIS/Terra and MODIS/Aqua.

3. Product description

The DSR and PAR products are available in two separate datasets: MCD18A1 (DSR) and MCD18A2 (PAR). MCD18A1 and MCD18A2 are gridded L3 products in MODIS sinusoidal map projection with 5km resolution. One product file is produced for one day over one MODIS sinusoidal land tile. Names of MCD18A1 and MCD18A2 follow file naming convention of standard MODIS products:

```
MCD18AX.AYYYYDDD.hHHvVV.006.PPPPPPPPPPPPP.hdf
where
X =1: DSR, 2: PAR
YYYY = year
DDD = day of year
HH = horizontal tile coordinate
VV = vertical tile coordinate
PPPPPPPPPPPPP = production date
```

3.1 MCD18A1 DSR product

MCD18A1 files are archived in Hierarchical Data Format V4 - Earth Observing System (HDF-EOS) format files. Each file contains global attributes (metadata) and scientific data sets (SDSs, data layers).

3.1.1 Metadata

MCD18A1 contains several global metadata attributes. The attributes include some basic information, such as `HDFEOSVersion`, `identifier_product_doi`, `identifier_product_doi_authority`. They also contain three global attributes used by standard MODIS products, known as EOS Data Information System (EOSDIS) Core System (ECS), namely, `CoreMetadata.0`, `ArchiveMetadata.0` and `StructMetadata.0`.

Besides, there are two attributes specifically used by MCD18A1: `Orbit_amount` and `Orbit_time_stamp`. Orbit_amount stores the count of the MODIS overpass covering the current day and tile. Orbit_time_stamp contains time information of each overpass in the format of `YYYYDDDHHMM`:

```
where YYYY = year
DDD = day of year
HH = hour
MM = minute
```

3.1.2 Data layers

Each MCD18A1 file contains two major types of scientific data sets: instantaneous DSR array for each individual MODIS overpass and 3-hour DSR array. Users should use “filling value” to check if DSR is successfully retrieved or not. No additional quality flag information is provided. The data sets are archived in 11 SDSs (Table 1).

Table 1. Summary of scientific data sets (data layers) in MCD18A1

Name	**Content**	**Dimension**	**Data type**	**Unit**	**Fill value**	**Valid range**
DSR	Instantaneous total DSR at MODIS overpass	n*240*240	32bit floating	W/m^2	-1	0-1400
Direct	Instantaneous direct DSR at MODIS overpass	n*240*240	32bit floating	W/m^2	-1	0-1400
Diffuse	Instantaneous diffuse DSR at MODIS overpass	n*240*240	32bit floating	W/m^2	-1	0-1400
GMT_0000_DSR	Total DSR at GMT 00:00	240*240	32bit floating	W/m^2	-1	0-1400
GMT_0300_DSR	Total DSR at GMT 03:00	240*240	32bit floating	W/m^2	-1	0-1400
GMT_0600_DSR	Total DSR at GMT 06:00	240*240	32bit floating	W/m^2	-1	0-1400
GMT_0900_DSR	Total DSR at GMT 09:00	240*240	32bit floating	W/m^2	-1	0-1400
GMT_1200_DSR	Total DSR at GMT 12:00	240*240	32bit floating	W/m^2	-1	0-1400
GMT_1500_DSR	Total DSR at GMT 15:00	240*240	32bit floating	W/m^2	-1	0-1400
GMT_1800_DSR	Total DSR at GMT 18:00	240*240	32bit floating	W/m^2	-1	0-1400
GMT_2100_DSR	Total DSR at GMT 21:00	240*240	32bit floating	W/m^2	-1	0-1400
ViewZenithAngle	View Zenith Angle of each MODIS overpass	n*240*240	32bit floating	degree	-1	0-90

n: the count of MODIS overpass, available from global attribute "Orbit_amount"
SDSs directly store DSR values. Scale and offset factors are not needed.

3.2 MCD18A2 PAR product

MCD18A2 files are organized in a manner similar to MCD18A1. The difference is that MCD18A2 contains PAR values instead of DSR values (Table 2).

Table 2. Summary of scientific data sets (data layers) in MCD18A2

Name	**Content**	**Dimension**	**Data type**	**Unit**	**Fill value**	**Valid range**
PAR	Instantaneous total PAR at MODIS overpass	n*240*240	32bit floating	W/m^2	-1	0-700
Direct	Instantaneous direct PAR at MODIS overpass	n*240*240	32bit floating	W/m^2	-1	0-700
Diffuse	Instantaneous diffuse PAR at MODIS overpass	n*240*240	32bit floating	W/m^2	-1	0-700
GMT_0000_PAR	Total PAR at GMT 00:00	240*240	32bit floating	W/m^2	-1	0-700
GMT_0300_ PAR	Total PAR at GMT 03:00	240*240	32bit floating	W/m^2	-1	0-700
GMT_0600_ PAR	Total PAR at GMT 06:00	240*240	32bit floating	W/m^2	-1	0-700
GMT_0900_ PAR	Total PAR at GMT 09:00	240*240	32bit floating	W/m^2	-1	0-700
GMT_1200_ PAR	Total PAR at GMT 12:00	240*240	32bit floating	W/m^2	-1	0-700
GMT_1500_ PAR	Total PAR at GMT 15:00	240*240	32bit floating	W/m^2	-1	0-700
GMT_1800_ PAR	Total PAR at GMT 18:00	240*240	32bit floating	W/m^2	-1	0-700

GMT_2100_ PAR	Total PAR at GMT 21:00	240*240	32bit floating	W/m^2	-1	0-700
ViewZenithAngle	View Zenith Angle of each MODIS overpass	n*240*240	32bit floating	degree	-1	0-90

n: the count of MODIS overpass, available from global attribute "Orbit_amount"

SDSs directly store PAR values. Scale and offset factors are not needed.

4. Obtaining MODIS DSR and PAR products

The MODIS DSR (MCD18A1) and PAR (MCD18A2) products are available to users free of charge. The products are archived at the Land Processes Distributed Active Archive Center (LP-DAAC). They can be ordered and downloaded through Earthdata Search (https://search.earthdata.nasa.gov/).

5. References

Huang, G., Ma, M., Liang, S., Liu, S., & Li, X. (2011). A LUT-based approach to estimate surface solar irradiance by combining MODIS and MTSAT data. *Journal of Geophysical Research*, *116*, D22201

Liang, S., Zheng, T., Liu, R., Fang, H., Tsay, S.C., & Running, S. (2006). Estimation of incident photosynthetically active radiation from Moderate Resolution Imaging Spectrometer data. *Journal of Geophysical Research-Atmospheres, 111*

Liu, R., Liang, S., He, H., Liu, J., & Zheng, T. (2008). Mapping photosynthetically active radiation from MODIS data in China. *Remote Sensing of Environment*, *112*, 998-1009

Lu, N., Liu, R., Liu, J., & Liang, S. (2010). An algorithm for estimating downward shortwave radiation from GMS-5 visible Imagery and its evaluation over China. *Journal of Geophysical Research-Atmospheres*, *115*, D18102, doi:18110.11029/12009JD013457

Zhang, X.T., Liang, S.L., Zhou, G.Q., Wu, H.R., & Zhao, X. (2014). Generating Global LAnd Surface Satellite incident shortwave radiation and photosynthetically active radiation products from multiple satellite data. *Remote Sensing of Environment*, *152*, 318-332

Zheng, T., Liang, S., & Wang, K.C. (2008). Estimation of incident PAR from GOES imagery. *Journal of Applied Meteorology and Climatology*, *47*, 853-868